Journal of Orthopaedic Translation 47 (2024) 97–104

Contents lists available at ScienceDirect

Journal of Orthopaedic Translation

journal homepage: www.journals.elsevier.com/journal-of-orthopaedic-translation

Original Article

Three-dimensional distribution of subchondral fracture lines in osteonecrosis of the femoral head

Yan-Bin Wu [a,b,1], Guang-Bo Liu [c,1], Huo Li [b,1], Jia-Zhou Wu [a,b], Jin-Shu Tang [b], Jian-Ting Ye [b], Ying-Jie Xiong [b], Xi-Wei Peng [b], Ze-Xian Liu [b], Yu-Zheng Lu [b], Cong-Cong Guan [b], Hao-Ye Meng [b], Xiao-Han Sun [b], Xin Wang [b], Ai-Yuan Wang [b], Zhe Zhao [b], Yuan Hu [b], Yu-Feng Liu [b], Li-Jun Sun [b], Ling Qin [d,**,2], Jiang Peng [a,b,*,2]

[a] Guizhou Medical University, Guizhou Province, 550004, PR China
[b] Institute of Orthopedics, The Fourth Medical Center of Chinese PLA General Hospital, Beijing Key Lab of Regenerative Medicine in Orthopedics, Key Laboratory of Musculoskeletal Trauma & War Injuries PLA, No. 51, Fucheng Road, Beijing, 100048, PR China
[c] Department of Orthopedics, Strategic Support Force Medical Center, No.9, Anxiangbeili, Beijing, 100101, PR China
[d] Musculoskeletal Research Laboratory, Department of Orthopaedics & Traumatology, The Chinese University of Hong Kong, Hong Kong, PR China

ARTICLE INFO

Keywords:
Collapse
Computed tomography
Osteonecrosis of the femoral head
Three-dimensional distribution

ABSTRACT

Objective: To investigate the characteristics of three-dimensional distribution of subchondral fracture lines on the surface of the osteonecrosis femoral head, and to discuss the underlying mechanisms that contribute to its collapse.

Methods: We retrospectively analyzed computed tomography (CT) images from 75 patients (comprising a total of 77 femoral heads) diagnosed with Association Research Circulation Osseous (ARCO) stage IIIA or IIIB femoral head necrosis. The three-dimensional structures of both the femoral head and the subchondral fracture line were reconstructed and subsequently fitted into normal femoral head model. A heat map of fracture line was generated to visualize its spatial distribution across the femoral heads surface.to observe its distribution. In addition to that, the femoral head was partitioned into four zones, and the frequency of each fracture line traversing different zones was calculated and analysed.

Results: Highest and lowest density of subchondral fracture lines was demonstrated in anterolateral and posterolateral zone respectively. and most sparse in posterolateral. Furthermore, the three-dimensional heat map of fracture lines highlighted their most frequent occurrence in the anterolateral area, particularly near the junction of the femoral head and neck. One fracture line may pass through multiple areas, passage frequencies for fracture lines was observed in zones I, II, III and IV for 66 times (85.7 %), 52 times (67.5 %), 25 times (32.5 %) and 46 times (59.7 %), respectively, with a significant difference between zone I and other zones ($P < 0.001$).

Conclusion: Subchondral fracture line of femoral head occurs most frequently in anterolateral femoral head, suggesting that the anterolateral part may be the initial location of collapse.

Translational potential of this article: We found that the subchondral fracture line was most frequently located anterolateral to the femoral head, suggesting that this may be the site of initiation of collapse. Furthermore, we propose an innovative method for analyzing and visualizing subchondral fracture distribution in femoral head necrosis in the form of fracture line heat maps. By doing so, we provide a valuable reference for physicians,

* Corresponding author. Area code: 010. Postal address: Institute of Orthopedics, The Fourth Medical Center of Chinese PLA General Hospital, No. 51, Fucheng Road, Beijing,100048, PR China.
** Corresponding author.
E-mail addresses: 412078439@qq.com (Y.-B. Wu), dr_liuguangbo@126.com (G.-B. Liu), lihuo301@126.com (H. Li), 675389398@qq.com (J.-Z. Wu), drtang304@126.com (J.-S. Tang), yejianting12@126.com (J.-T. Ye), xyj353594843@163.com (Y.-J. Xiong), 3297269227@qq.com (X.-W. Peng), 863699617@qq.com (Z.-X. Liu), 493074156@qq.com (Y.-Z. Lu), 1710944@mail.nankai.edu.cn (C.-C. Guan), menghaoye@126.com (H.-Y. Meng), 384347863@qq.com (X.-H. Sun), wangx126@126.com (X. Wang), wangaiyuan301@126.com (A.-Y. Wang), applezztj@163.com (Z. Zhao), dr_huyuan@163.com (Y. Hu), drmartinliu@163.com (Y.-F. Liu), ljsunstudy@163.com (L.-J. Sun), lingqin@cuhk.edu.hk (L. Qin), pengjiang301@126.com (J. Peng).
[1] Co-first author: The first three authors contributed equally to this work and are considered
[2] Co-first authors: The last two authors (Jiang Peng and Ling Qin) are considered corresponding authors

https://doi.org/10.1016/j.jot.2024.06.004
Received 22 January 2024; Received in revised form 8 April 2024; Accepted 3 June 2024

enabling them to enhance their management strategies for femoral head necrosis. Ultimately, this approach holds the promise of significantly improving the prognosis and outcomes for patients afflicted with this condition.

1. Introduction

Osteonecrosis of the Femoral Head (ONFH), arising from compromised blood supply to the femoral head and leading to bone cell and marrow death, poses a formidable orthopedic challenge [1,2]. Subsequent collapse can trigger secondary osteoarthritis (OA), accompanied by severe pain and dysfunction [3]. Early intervention to prevent femoral head collapse is pivotal in managing this condition.

The crux of successful preservation treatment hinges upon unraveling the intricate mechanism behind femoral head collapse. Existing literature posits two pivotal factors: the diminution of bone structural strength due to osteoclast activity, and the stress concentration at the interface between the indurated necrotic region and the adjacent necrotic bone [4–6]. These combined forces hold the potential to precipitate femoral head collapse. However, despite extensive research, a consensus on the precise collapse mechanism in ONFH remains elusive [7–9]. Notably, subchondral bone fractures emerge as a critical juncture - once they occur, femoral head collapse becomes inevitable, acting as a triggering event [10]. Consequently, meticulous scrutiny of subchondral bone fracture occurrence and progression assumes paramount importance in elucidating the collapse mechanism. While prior studies have identified the prevalence of subchondral bone fractures at the lateral edge of the necrotic area [8], these investigations predominantly rely on histological data or partial CT images, precluding a comprehensive three-dimensional mapping of subchondral bone fractures across the femoral head's surface.

The concept of fracture line distribution map was pioneered to the analysis of scapular fracture patterns by Bryan M. Armitage and colleagues in 2009 [11]. Through computer image simulation, they superimposed multiple instances of fracture lines onto a normal bone model, effectively reconstructing the intricate morphology of fractures. This approach equips medical practitioners with a more intuitive, three-dimensional comprehension of fractures, thereby enhancing clinical decision-making for its prevention and treatment. Building upon this foundation, our research endeavors to introduce this widely utilized approach from trauma orthopedics into analyzing the three-dimensional distribution of subchondral fractures within the osteonecrosis femoral head. We hope to gain a more intuitive and precise understanding of the collapse area and illuminate the elusive mechanism underlying femoral head collapse.

In summary, the purpose of this study is to analyze the distribution characteristics of the fracture lines across the surface of the femoral head by employing three-dimensional heatmap and femoral head zoning method. By doing so, our ultimate goal is to unravel the elusive mechanism underpinning femoral head collapse. These insights hold the potential to serve as a foundational basis for enhancing clinical strategies in the prevention and treatment of ONFH.

2. Materials and methods

2.1. Ethnic approvement

Ethics Approval No. 2023KY090-KS001 was obtained from the Clinical Trial Medical Ethics Committee at the Fourth Medical Center of PLA General Hospital before the study starts. The principles stated in the Declaration of Helsinki was abided. All participants were duly informed about the study's objectives and content, and informed consent documents were signed.

2.2. Patient recruitment and imaging protocol

CT scans of patients diagnosed with Association Research Circulation Osseous (ARCO) stage [12] IIIA or IIIB ONFH between January 2018 and December 2022 underwent meticulous evaluation. All CT images adhered to stringent criteria: a scanning layer thickness of $\leq$1 mm, a slice increment of $\leq$0.6 mm, and a pixel size of $\leq$0.8 mm. Exclusion criteria encompassed patients with a history of hip joint trauma or surgery, as well as those presenting concurrent osteoarthritis, congenital

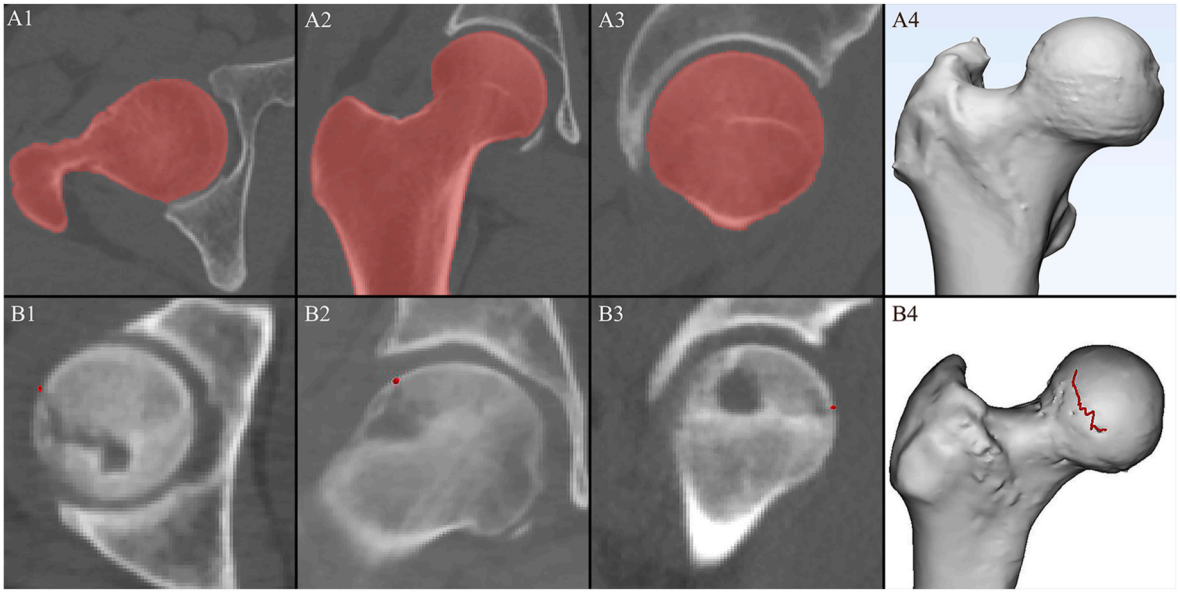

Figure 1. Reconstruction of template femoral head and subchondral fracture line. Areas of interest in CT images were colored in red (A1-A3). The contours of a healthy femoral head was derived through a combination of semi-automatic software tools and manual refinement (A4). Subchondral fracture lines were traced layer by layer from axial, coronal and sagittal positions(B1–B3), the red dots in B1–B3 are markers depicting the subchondral fracture line. (B4) Fracture line projection after reconstruction.

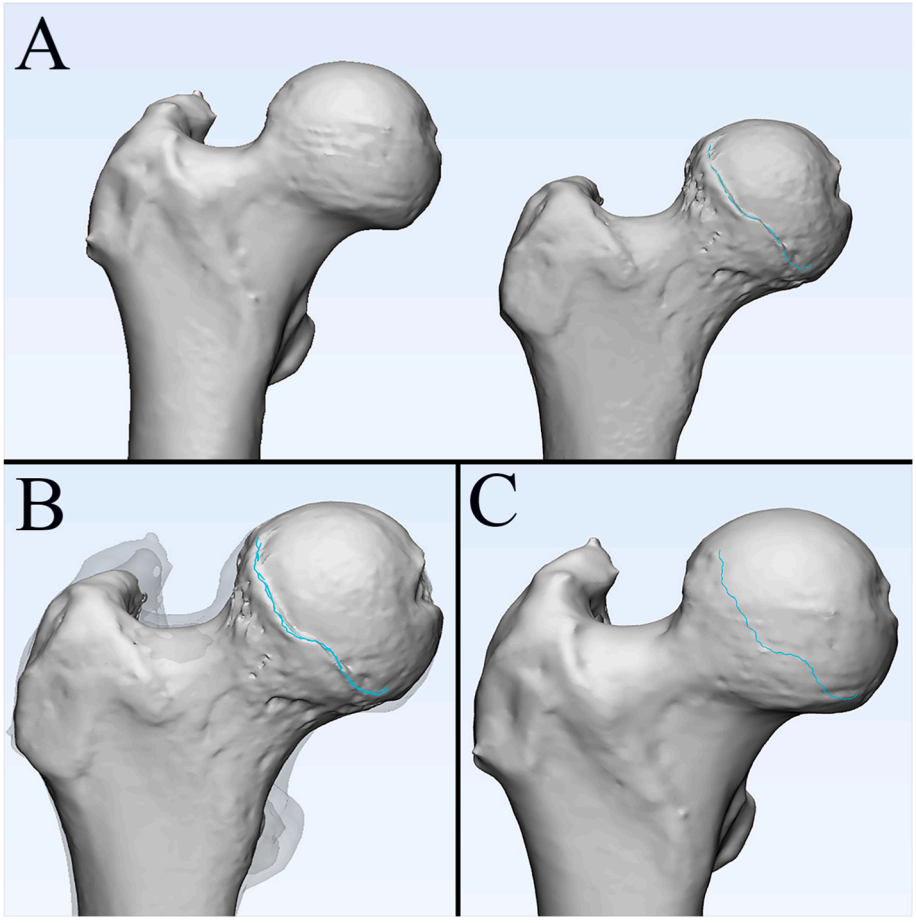

Figure 2. Fracture line projection. A. Superimpose the reconstructed 3D model of collapsed femoral head onto the template femoral head; B. Through adjustment of position, size and other parameters, merging the 2 femoral head models and project the fracture line onto the template; C. The fracture line was reconstructed on the template femoral head.

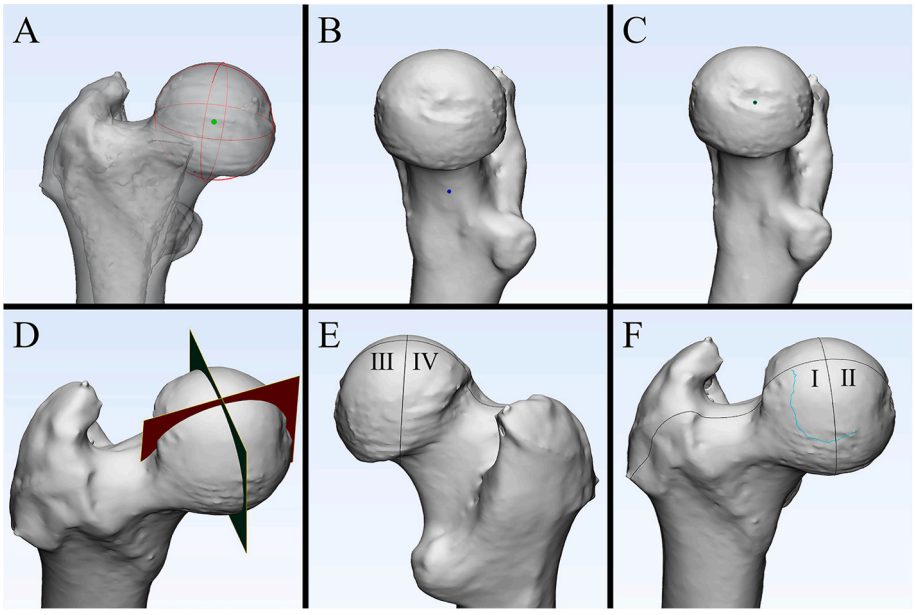

Figure 3. Femoral head partitioning method. Figure A: The green dot corresponds to the center of the femoral head. Figure B: The blue dot represents the midpoint of the femoral calcar. Figure C: Another blue dot signifies the midpoint of the concavity within the femoral head. In figure D, two perpendicular planes were constructed by intersecting through these three points. Femoral head surface was divided into 4 zones: Zone III (Figure E): Represents the posteromedial region. Zone IV (Figure E): Corresponds to the posterolateral region. Additionally, in Figure F: Zone I: Encompasses the anterolateral region. Zone II: Refers to the anteromedial region. The green curve is the projection of one fracture line, passing through Zone I and II simultaneously.

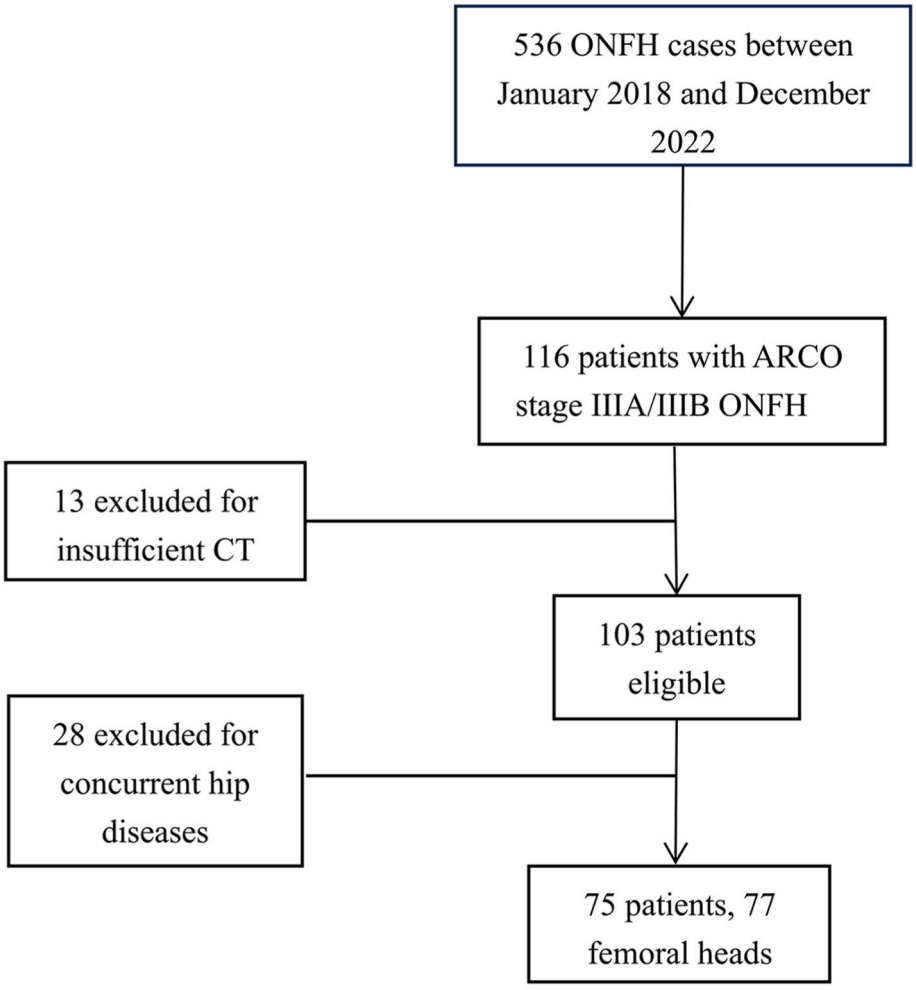

Figure 4. Patient Enrollment Flowchart. Final group includes 75 patients with 77 femoral heads. ARCO =Association Research Circulation Osseous; ONFH=Osteonecrosis of the Femoral Head; CT=Computed tomography.

hip joint disease, or other hip joint pathologies.

2.3. Three-dimensional reconstruction of the femoral head and subchondral fracture lines

The CT data of a normal left hip joint were imported into Mimics software (version 21.0, Materialise, Leuven, Belgium). First, a rough structure of the femoral head was derived using the tool based on Hounsfield units (related to intensity). Then the details of the femoral head were refined by manually drawing the femoral head contour on each plane (Fig. 1A). Finally, by employing Mimics, the acquired images underwent a smoothing process to achieve optimal homogeneity and anatomically three-dimensional similarity.

Similarly, the three-dimensional images of the collapsed femoral heads were obtained in the same way (Fig. 1 B1-4). Notably, the precise position of subchondral fracture was depicted onto the femoral head surface based on the CT image, effectively reconstructing the projection of the fracture line within the femoral head surface.

2.4. Fracture line alignment and visualization

The reconstructed femoral head and fracture lines were imported into the 3-matic Research software (version 13.0, Materialise, Leuven, Belgium). Through adjustments of parameters such as position and size, the model was aligned with the template femoral head (Fig. 2A). If the femoral head is on the left side, it is converted to the right side by the mirror conversion function. To enhance visibility, the transparency of the template femoral head was adjusted, rendering both the collapsed femoral head and the fracture lines discernible. This facilitated the depiction of the fracture lines on the template femoral head, effectively tracing their projection onto the collapsed femoral head (Fig. 2B). Finally, the collapsed femoral head and fracture line were hidden, and the template femoral head was restored to the opaque state, and the fracture line was reconstructed on the template femoral head (Fig. 2C).

2.5. Heat map analysis of subchondral fracture lines of femoral heads

To gain deeper insights into the spatial distribution of subchondral fracture lines within the femoral head, the superimposed fracture line map was imported into E−3D Medical Modeling and Design System x64 (Universal version 20.03; Nanjing Huiqing Information Technology Co., Ltd , Nanjing City, Jiangsu Province, China) and a three-dimensional heat map of the femoral head surface was generated. We defined fracture lines involving only two areas below as shorter fracture lines and performed heat map analysis separately.

2.6. Spatial distribution of the subchondral bone fracture lines within the femoral heads

To elucidate the distribution patterns of subchondral fracture lines across the surface of the femoral head, the femoral head was divided into four zones according to our innovative zoning approach study [13],but

Table 1
The baseline characteristics and demographics of the study population.

Variable	Outcome
Age (year, mean ± SD)	37.1 ± 11.3
Gender (Male/Female)	61/16
Side (Left/Right)	51/26
ARCO (Stage IIIA/IIIB)	
IIIA (%)	60(77.92)
IIIB (%)	17 (22.08)
Aetiology	
Steroid (%)	30 (38.96)
Alcohol (%)	25 (32.47)
Idiopathic (%)	22 (28.57)

ARCO, Association Research Circulation Osseous. SD, Standard Deviation.

A-D is changed to I-IV zones. Specifically, we delineated the femoral head into four distinct zones (I-IV) using key landmarks: the center of the femoral head, the fovea of the femoral head, and the center of the calcar femoris (Fig. 3). Given that fracture lines may intersect multiple zones simultaneously, statistical comparisons of their distribution become intricate. Instead, we quantified the frequency of fracture lines traversing each zone and subjected the data to multiple chi-square tests to assess significant differences in their distribution probabilities.

2.7. Statistical analysis

We used (x- ± s) to describe continuous variables and percentages for categorical variables. Multiple chi-square test was used to analyze the distribution frequency of fracture lines in each zone of the femoral head. SPSS 23.0 was used to analyze the data.

3. Results

3.1. Patients demographics

Following the inclusion and exclusion criteria, a total of 75 patients with 77 femoral heads were included in this study (Fig. 4). The demographic of the selected patients was shown in Table 1.

3.2. Distribution patterns of subchondral fracture lines

The subchondral fracture lines were densely distributed on the anterior side (zones I, II) of the femoral head and sparsely distributed on the posterior side. It can be intuitively seen that the distribution in zone I is the most dense, and the number of fracture lines significantly reduces behind the femoral head (Fig. 5).

3.3. Heat map of subchondral fracture lines

The heat map of distribution patterns of subchondral fracture lines was generated using E−3D Medical Modeling and Design System x64 (Universal version 20.03; Nanjing Huiqing Information Technology Co., Ltd , Nanjing City, Jiangsu Province, China) . The relative frequency of the fracture lines was represented using different colors (blue to red indicated the incidence from low to high, and the impact distance was 2 mm around the long axis of the fracture line). It was revealed clearly that the subchondral fracture lines of the femoral head appeared on all four surfaces of the femoral head. The anterior fracture line had the highest distribution frequency, followed by the superior and medial

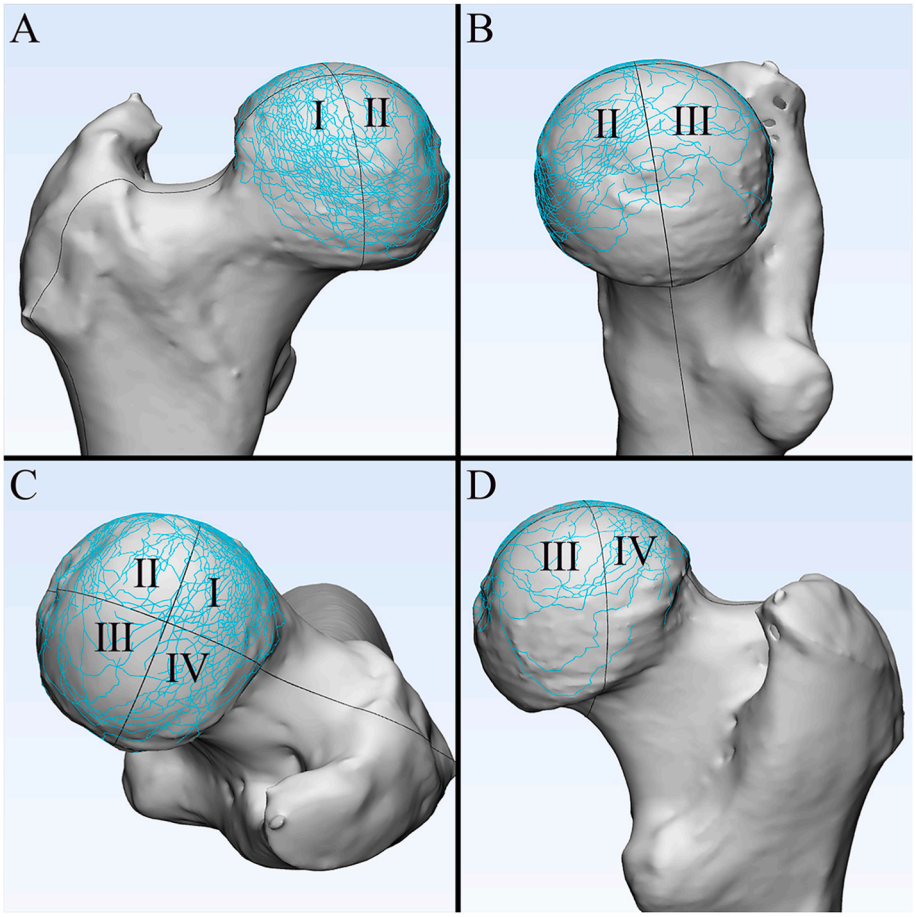

Figure 5. Subchondral fracture lines distribution of femoral head. *A. anterior* view; B. view from above; C. medial view; d. Posterior view.

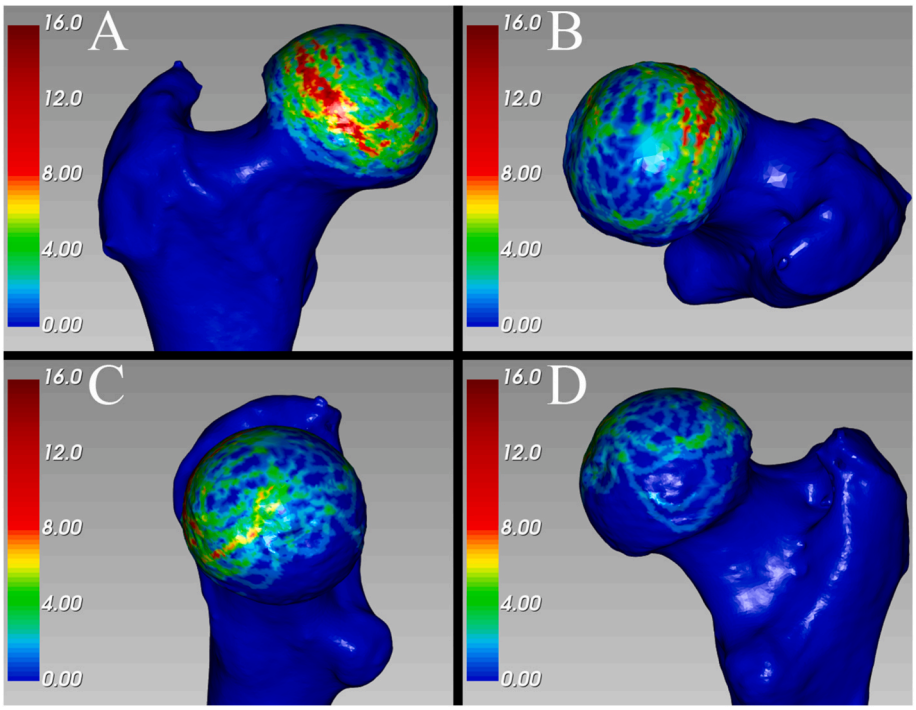

Figure 6. Heat Map of the distribution of subchondral fracture line of femoral head. *A. anterior* view; B. view from above; C. medial view; D. Posterior view.

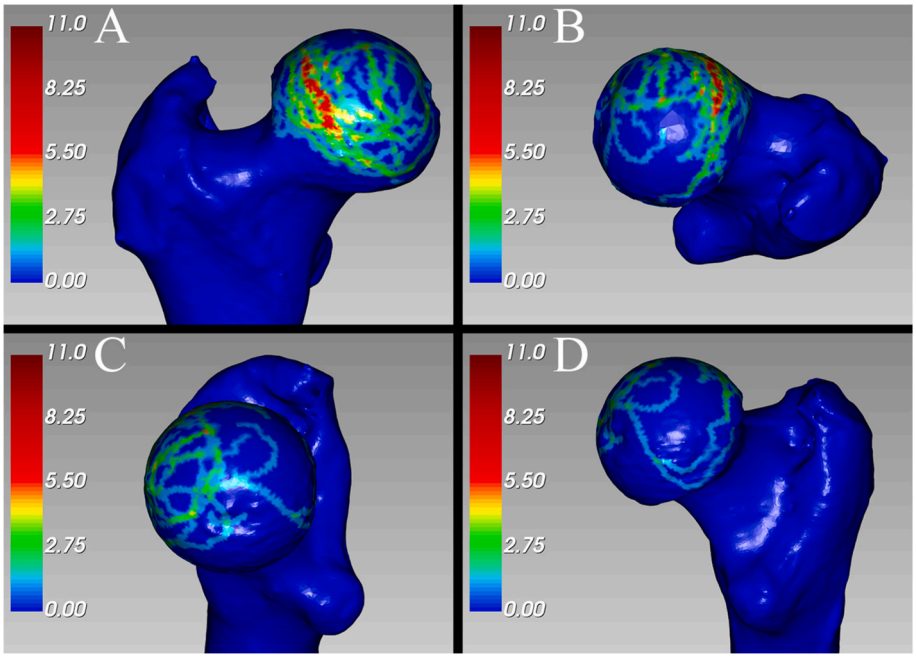

Figure 7. map of subchondral fracture line distribution involving two or fewer areas. *A. anterior* view; B. view from above; C. medial view; D. Posterior view.

Table 2
Distribution of femoral head fracture lines frequency across four zones (I-IV).

Zone	Number of fracture lines (Yes)	Percentage with fracture lines (Yes)	Number without fracture lines (No)	Percentage without fracture lines (No)	Total	P-value (compared to zone I)	P-value (compared to previous zone)
I	66	85.7 %	11	14.3 %	77	N/A	N/A
II	52	67.5 %	25	32.5 %	77	<0.001	<0.001
III	25	32.5 %	52	67.5 %	77	<0.001	<0.001
IV	46	59.7 %	31	40.3 %	77	<0.001	0.001
Total	189	61.4 %	119	38.6 %	308	N/A	N/A

I, Anterolateral; II, Anteromedial; III, Posteromedial; IV, Posterolateral. "N/A″ stands for "Not Applicable".

sides, with the posterior side having the lowest frequency. The anterolateral side of the femoral head, close to the head-neck junction, had the highest distribution frequency of the fracture line, represented by the red area, with its running direction from superior side to the anterolateral side (Fig. 6).

In order to explore the stepwise characteristics of earlier subchondral fracture lines, we defined the fracture lines involving only two areas below as the shorter fracture lines (43 lines), and reconstructed their 3D distribution heat map (Fig. 7). The red area representing the highest frequency of fracture line distribution was still on the anterolateral side of the femoral head (Fig. 7).

3.4. Distribution of fracture lines in different zones of the femoral head

Table 2 shows the distribution of the frequency of fracture lines occurring in the four zones of the femoral head. The frequencies of 77 fracture lines in zone I, II, III and IV were 66 (85.7 %), 52 (67.5 %), 25 (32.5 %) and 46 (59.7 %), respectively. The frequency of fracture lines in zone I was significantly higher than that in other zones ($P < 0.001$). There was no significant difference in the frequency of fracture lines between zone II and zone IV($P = 0.315$), but the frequency of fracture lines in zone II was higher than that in zone III ($P < 0.001$).

4. Discussion

To the best of our knowledge, this study is the first to investigate the distribution of subchondral fracture lines of the femoral head at three-dimensional level. Based on the results of our 3D reconstruction and heat map analysis, it was found that the area with the highest frequency of fracture line distribution was the anterolateral side of the femoral head. The heat map analysis of fracture line showed that the densest area was distributed in a linear arc from the superior lateral side of the femoral head to the anterolateral side. In addition, the statistical results of our subregional study of subchondral fracture line distribution also supported this view, with a statistically significant difference in the probability of fracture line passing through the anterolateral zone compared to the other three zones.

The crescent sign on the plain film was considered the first sign of the formation of subchondral fractures of the femoral head. Numerous scholars have conducted relevant research on the collapse mechanism of the femoral head [12]. Some speculation has been well recognized by most scholars: 1. Shear stress effect at the junction between the necrotic and healthy area [8]; 2. Increased bone absorption at the junction between the necrotic and healthy area [14]. 3. Cumulative effect of unhealed fatigue fractures in necrotic areas [5]. These theories all suggest that necrosis of the femoral head changes the mechanical distribution on the surface of the femoral head, leading to the eventual collapse. For example, Karasuyama et al. [4]. found through finite element analysis that both shear stress and shear strain tend to be concentrated on thickened bone trabeculae at the boundary along with the progression of sclerotic changes. Their results suggest that the boundary of sclerotic change may be the starting point of the fracture. Regarding the starting point of collapse, a recent study on the three-dimensional structure of the entire femoral head collapse in the early and late stages based on micro-CT found that [10]: In the early collapse stage of ONFH, all initial fractures occur between the separated bone resorption areas in the anterior upper part of the femoral head, and their findings suggest that bone resorption around the repair area is the initiating factor for subchondral fractures in ONFH. While previous studies focused on the position relationship between the local lesion area of the femoral head and the eventual occurrence of subchondral fracture. our study aims to explore the position relationship between the subchondral fracture line and the overall surface of the femoral head. Our research results show that the anterolateral side of the femoral head is the fracture line prone area.

It is well known that once the femoral head begins to collapse, most of the ONFH will continue to develop and eventually enter ARCO stage IV [15]. As the collapse progresses, the fracture lines will gradually extend and even join in a circle (Fig. 8). The fracture line is actually the shape of the collapse boundary of the fracture. Moreover, in the reconstructed three-dimensional heat map of fracture line distribution involving only two areas below, the area with the highest frequency of fracture lines is still located on the anterolateral side of the femoral head (Fig. 7). Consequently, this study suggests that the anterolateral part may be the initial location of collapse. To prove this point, the ideal approach would involve continuous monitoring of patients from the initial appearance of a subchondral fracture line without implementing any interventions, which is evidently unethical.

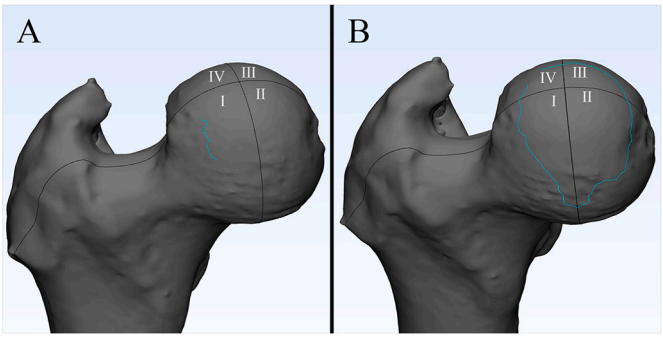

Figure 8. The subchondral fracture lines of the femoral head after reconstruction in two cases. A. An early-stage fracture line in femoral head collapse (marked by the green line). B. A late-stage fracture line in femoral head collapse (marked by the green line). In figures A and B, I, II, III, and IV represent four different regions on the surface of the femoral head.

Previous study on the distribution of cystic lesions in ONFH conducted by our team [13] showed that cystic lesions were mostly located in the anterolateral part of the femoral head, which was coincide with the distribution patterns of the subchondral fracture line in this study. Other studies on cystic lesions in ONFH also suggested that cystic lesions played an important role in aggravating the progression of femoral head collapse [16]. These coincidences might suggest potential relationship between the cyst formation and subchondral fracture, but the causality remains to be elucidated.

The anterolateral hemisphere of the femoral head suffers a constant and rapid switch of high peak and low stress as its coverage by the acetabulum changes at normal gait [17,18]. As a result, the anterolateral hemisphere of the femoral head is subjected to high stress of the acetabulum, resulting in fractures and collapse of the femoral head after necrosis. Similar findings from our study suggest that subchondral fractures are more likely to occur at the anterolateral side of the femoral head. In our study, the distribution of fracture lines on the surface of the femoral head was reconstructed in three dimensions, which enabled clinicians to have a more intuitive understanding of the high incidence area of femoral head collapse.

Although there is still controversy about the optimal treatment for ONFH, it is generally believed that active treatment before femoral head collapse can greatly improve the success rate of joint-preserving [19,20]. It is well known that the location of the lateral border of the necrotic area affects the fate of ONFH [3], because the lateral border of the necrotic area is distributed in the front and rear of the femoral head. Combined with the results of our study that the fracture line mainly occurs in the anterolateral part, so it is reasonable to believe that the mechanical protection in front of the necrotic area of the femoral head during the operation is essential to prevent or delay the progression of the collapse of the femoral head.

The results of a study about gait analysis of hip joint conducted by showed that during a gait cycle, the acetabular contact stress is mainly distributed in the anterolateral region of the top of the acetabulum and the top of the femoral head, and the stress of the acetabulum moves from

anterior to the posterior column of the acetabulum [21,22]. The anterolateral part of the top of the femoral head bears the most concentrated force in the early stage. This is precisely the area where the subchondral fracture line is prone to occur in our study. Therefore, according to our results, reducing the pressure on the femoral head in the early stage of the gait cycle will help to prevent the occurrence of anterolateral subchondral fractures in ONFH and provide a valuable reference for the rehabilitation treatment of ONFH.

Certain limitations do exist in this study. First, our sample size was relatively smaller, and further multicenter, larger sample size studies should be carried to acquire a more comprehensive result; secondly, earlier subchondral fracture lines are hard to be detected without the help with Micro-CT, but what we used was sufficient to tell the story. Finally, we only studied the distribution of subchondral fracture lines and discussed the possible causes, but did not conduct further verification of the possible mechanism. It is necessary to study the relationship between subchondral fracture lines and structural changes around the femoral head in the future.

5. Conclusion

Subchondral fracture line of femoral head occurs most frequently in anterolateral femoral head, suggesting that the anterolateral part may be the initial location of collapse.

Conflicts of interest statement

The author(s) have no conflicts of interest relevant to this article.

Declaration of interest

Declarations of interest: none.

Funding

This study was funded by the National Key Research and Development Program of China (2022VFB3804303) and the National Natural Science Foundation of China (81972047).

Funding/support statement

This research did not receive any specific grant from funding agencies in the public, commercial, or not-for-profit sectors, and no material support of any kind was received.

Compliance with ethical standards

This article was approved by the Clinical Trial Medical Ethics Committee at the Fourth Medical Center of PLA General Hospital (2023KY090-KS001)

Appendix A. Supplementary data

Supplementary data to this article can be found online at https://doi.org/10.1016/j.jot.2024.06.004.

References

[1] Larson E, Jones LC, Goodman SB, Koo KH, Cui Q. Early-stage osteonecrosis of the femoral head: where are we and where are we going in year 2018? Int Orthop 2018;42(7):1723–8 [eng].
[2] Hines JT, Jo WL, Cui Q, Mont MA, Koo KH, Cheng EY, et al. Osteonecrosis of the femoral head: an updated review of ARCO on pathogenesis, staging and treatment. J Kor Med Sci 2021;36(24):e177 [eng].
[3] Ohzono K, Saito M, Takaoka K, Ono K, Saito S, Nishina T, et al. Natural history of nontraumatic avascular necrosis of the femoral head. J Bone Joint Surg Br 1991;73 (1):68–72 [eng].
[4] Karasuyama K, Yamamoto T, Motomura G, Sonoda K, Kubo Y, Iwamoto Y. The role of sclerotic changes in the starting mechanisms of collapse: a histomorphometric and FEM study on the femoral head of osteonecrosis. Bone 2015;81:644–8 [eng].
[5] Bullough PG, DiCarlo EF. Subchondral avascular necrosis: a common cause of arthritis. Ann Rheum Dis 1990;49(6):412–20 [eng].
[6] Quan H, Ren C, He Y, Wang F, Dong S, Jiang H. Application of biomaterials in treating early osteonecrosis of the femoral head: research progress and future perspectives. Acta Biomater 2023;164:15–73 [eng].
[7] Brown TD, Mutschler TA, Ferguson Jr AB. A non-linear finite element analysis of some early collapse processes in femoral head osteonecrosis. J Biomech 1982;15 (9):705–15 [eng].
[8] Motomura G, Yamamoto T, Yamaguchi R, Ikemura S, Nakashima Y, Mawatari T, et al. Morphological analysis of collapsed regions in osteonecrosis of the femoral head. J Bone Joint Surg Br 2011;93(2):184–7 [eng].
[9] Zheng GS, Qiu X, Wang BJ, Zhao DW. Relationship between blood flow and collapse of nontraumatic osteonecrosis of the femoral head. J Bone Joint Surg Am 2022;104(Suppl 2):13–8 [eng].
[10] Hamada H, Takao M, Sakai T, Sugano N. Subchondral fracture begins from the bone resorption area in osteonecrosis of the femoral head: a micro-computerised tomography study. Int Orthop 2018;42(7):1479–84 [eng].
[11] Armitage BM, Wijdicks CA, Tarkin IS, Schroder LK, Marek DJ, Zlowodzki M, et al. Mapping of scapular fractures with three-dimensional computed tomography. J Bone Joint Surg Am 2009;91(9):2222–8 [eng].
[12] Yoon BH, Mont MA, Koo KH, Chen CH, Cheng EY, Cui Q, et al. The 2019 revised version of association research circulation osseous staging system of osteonecrosis of the femoral head. J Arthroplasty 2020;35(4):933–40 [eng].
[13] Liu GB, Li R, Lu Q, Ma HY, Zhang YX, Quan Q, et al. Three-dimensional distribution of cystic lesions in osteonecrosis of the femoral head. J Orthop Translat 2020;22: 109–15 [eng].
[14] Li W, Sakai T, Nishii T, Nakamura N, Takao M, Yoshikawa H, et al. Distribution of TRAP-positive cells and expression of HIF-1alpha, VEGF, and FGF-2 in the reparative reaction in patients with osteonecrosis of the femoral head. J Orthop Res 2009;27(5):694–700 [eng].
[15] Xia T, Wei W, Zhang C, Ji W, Shen J. [Hip preservation experience of avascular necrosis of femoral head according to China-Japan Friendship Hospital classification]. Zhongguo Xiu Fu Chong Jian Wai Ke Za Zhi 2020;34(1):10–5 [chi].
[16] Gao F, Han J, He Z, Li Z. Radiological analysis of cystic lesion in osteonecrosis of the femoral head. Int Orthop 2018;42(7):1615–21 [eng].
[17] Moya-Angeler J, Gianakos AL, Villa JC, Ni A, Lane JM. Current concepts on osteonecrosis of the femoral head. World J Orthoped 2015;6(8):590–601 [eng].
[18] Sissons HA, Nuovo MA, Steiner GC. Pathology of osteonecrosis of the femoral head. A review of experience at the Hospital for Joint Diseases, New York. Skeletal Radiol 1992;21(4):229–38 [eng].
[19] Mont MA, Salem HS, Piuzzi NS, Goodman SB, Jones LC. Nontraumatic osteonecrosis of the femoral head: where do we stand today?: a 5-year update. J Bone Joint Surg Am 2020;102(12):1084–99 [eng].
[20] Ando W, Sakai T, Fukushima W, Kaneuji A, Ueshima K, Yamasaki T, et al. Japanese Orthopaedic Association 2019 Guidelines for osteonecrosis of the femoral head. J Orthop Sci 2021;26(1):46–68 [eng].
[21] Xiong B, Yang P, Lin T, Xu J, Xie Y, Guo Y, et al. Changes in hip joint contact stress during a gait cycle based on the individualized modeling method of "gait-musculoskeletal system-finite element". J Orthop Surg Res 2022;17(1):267 [eng].
[22] Wang G, Huang W, Song Q, Liang J. Three-dimensional finite analysis of acetabular contact pressure and contact area during normal walking. Asian J Surg 2017;40(6): 463–9 [eng].